

Short note

Inflow conditions for the large eddy simulation of turbulent boundary layers: A dynamic recycling procedure

Kunlun Liu *, Richard H. Pletcher

Department of Mechanical Engineering, 2025 Black Engineering Building, Iowa State University, Ames, IA 50011, United States

Received 1 June 2005; received in revised form 23 December 2005; accepted 5 April 2006

Available online 5 June 2006

Keywords: Inflow conditions; Turbulent boundary layers; Recycling method

1. Introduction

The simulation of turbulent boundary layers requires quite detailed inflow information since the resolved flow is unsteady and three-dimensional. Rather than simulating laminar and transitional regions arising near a leading edge, it is often more computationally efficient to formulate a fully turbulent inflow condition. To date, three types of methods for creating appropriate inflow conditions have been suggested: the random fluctuation method [1], the matching database method [2], and the recycling and rescaling method [3,4]. The classification of those methods is based on their different treatments of the mean profile and fluctuations at inflow. Among those methods, the recycling method appears to establish a turbulent shear flow with a fairly short inlet buffer zone and provides accurate downstream profiles.

The recycling method was introduced by Spalart [3]. Lund et al. [4] further developed this concept, and introduced a rescaling idea. In their implementation, instantaneous profiles at a specific station were recycled to the inlet at each numerical step after rescaling. This rescaling was based on the similarity laws of the boundary layer: the law of the wall in the inner part and the defect law in the outer part of the boundary layer.

If the rescaling starts by using downstream data that are far from a correct turbulent state, the skin friction may decrease with time and make the achievement of the desired inflow turbulent state very difficult. The difficulty results from the coupling of the initial and inflow condition during the starting transient. Since the non-physical transient solution relevant to the initial fields are recycled to the inlet, this procedure causes such a coupling in the early part of the simulation. Although it is believed that, after a long time evolution, the flow will become independent of the initial conditions. However, the initial condition will influence the length of the starting transient. To overcome the problem arising from unsuitable initial conditions, Lund et al. [4] suggested making a correction to the resolved velocities during the early part of simulation. Spille-Kohoff

* Corresponding author. Tel.: +1 515 294 6954.
E-mail address: kliu@iastate.edu (K. Liu).

and Kaltenbach [5] suggested adding a source term to the resolved equation based on the desired Reynolds stress.

The present paper proposes an advance to the method of Lund et al. [4] for the simulation of turbulent boundary layers subjected to zero pressure gradient. In the present method, the recycling plane is dynamically positioned according to the downstream instantaneous field. And the weighting parameter in Lund et al.'s [4] rescaling method is modified. With this inlet generation technique, the first and second order statistics compare well with recent experimental and DNS results and the size of the starting transient appears to be reduced.

2. The improved rescaling method

The rescaling method has a weak point: it is difficult to rapidly generate correct downstream turbulence to use for recycling if the initial inflow conditions are not accurate. Similarly, it is difficult to improve the inflow conditions by recycling a profile that is far from correct. If the initial conditions are not well posed, the interior Reynolds stress may continuously decay. This tendency toward decay is hard to remedy by the above rescaling treatment. Moreover, if the initial conditions are not proper, i.e., the correct large eddies have not been produced in the interior at the right time, the mean profiles and velocity rms profiles may not be correct. Hence, similarity laws are not strictly applicable. The method of Lund et al. [4], which is based on an assumption that the recycling profile and the inflow profile data satisfy the similarity law, will result in a long transient until equilibrium is established. The rescaling method proposed by Lund et al. is promising, but can be improved by a reduction in the start-up transient associated with the method. Furthermore, a suitable recovery from the skin-friction decay could not be achieved in several hundred time units ($\frac{\delta_d}{U_\infty}$) when Lund et al.'s scheme was used with a fully implicit numerical scheme. This provided motivation for the present study.

2.1. The dynamic recycling

The convective speed of turbulent structures in the turbulent boundary layer with zero pressure gradient varies with the distance from the wall, and this speed is roughly proportional to the streamwise velocity. Therefore, the fluid structures generated by the inflow conditions will take some time to reach the recycling plane. Our numerical experience showed that the structures evolving from the initial condition tend to decay, but the structures produced by the rescaled inflow conditions maintain the balance of turbulent production and dissipation quite well, provided that the mean profile and Reynolds stresses of the inflow profiles appear steady and accurate. Therefore, in order to efficiently and accurately establish the turbulent boundary layer, we suggest dynamically selecting the recycling plane so that the recycling plane is kept within the turbulent region produced by inflow conditions during the early part of the simulation, since the similarity laws can be satisfied in this region. The proposed recycling plane is located by:

$$X_2 = X_1 + \min(X_{\text{tag}} - X_1, \alpha U_b \max(0, (t - t_0))) \quad (1)$$

where X_2 is the recycling location, X_{tag} is the desired recycle station when the numerical domain is completely occupied by the turbulent structures produced by the inlet conditions, X_1 is the starting location of the recycling plane, t is non-dimensional time, U_b is the bulk velocity, which is an average velocity cross the boundary layer, and t_0 is the time at which the leading edge of the convected flow generated at the inlet reaches station X_1 . Eq. (1) indicates that the recycling plane stays at station X_1 from $t = 0$ up to $t = t_0$, at which time the structures generated by the inlet conditions are expected to pass through station X_1 except for the viscous sublayer, and then the recycling plane moves downstream with the speed αU_b until it reaches the desired location X_{tag} . After that, the recycling plane will remain fixed for the remainder of the simulation. The purpose of this is to keep the recycling plane inside the convective region influenced by the inflow conditions to achieve accurate first and second order statistics. In our simulation, $X_1 = 10\delta_d$, $\alpha = 0.5$, and $t_0 = 10$ where δ_d is the displacement thickness at the inlet.

When the turbulence is fully established, the recycling plane should be fixed. Thus, this dynamic process is stopped when the recycling plane reaches X_{tag} . Considering that the dynamic recycling method has a different transient compared with the fixed recycling method, an interesting question that needs to be answered is

whether this dynamic recycling would break up the turbulent structures. Guarini et al.'s [6] two-point correlation analysis shows that if the recycling station is far enough from the inlet, the recycled fluctuations will be independent of the inlet fluctuations. This feature enables us to set up an inlet condition based on the recycling of downstream profiles without breaking up the fast moving or slow moving structures by keeping the recycling plane some distance from the inlet. Experiments conducted by Smith and Metzler [7] observed that the streaky structure extends over a streamwise distance of $\Delta L_x^+ > 1000$, and Iritani et al. [8] found that the thermal streaky structure extends over a streamwise distance of $\Delta L_x^+ > 1000$ also. Those studies implied that keeping a large enough distance is necessary when recycling. Thus, we start the recycling from the station X_1 , but not from the inlet.

2.2. The inflow conditions

The inflow conditions proposed by this paper are:

$$U_{\text{inlt}}^{\text{inner}}(y_{\text{inlt}}^+) = \gamma U_{\text{recy}}(y_{\text{inlt}}^+) + \gamma_1 U'_{\text{recy}}(y_{\text{inlt}}^+, z, t) \quad (2)$$

$$T_{\text{inlt}}^{\text{inner}}(y_{\text{inlt}}^+) = \gamma T_{\text{recy}}(y_{\text{inlt}}^+) + \gamma_1 T'_{\text{recy}}(y_{\text{inlt}}^+, z, t) + T_{w,\text{inlt}} - \gamma T_{w,\text{recy}} \quad (3)$$

$$U_{\text{inlt}}^{\text{outer}}(\eta_{\text{inlt}}) = \gamma U_{\text{recy}}(\eta_{\text{inlt}}) + \gamma_1 U'_{\text{recy}}(\eta_{\text{inlt}}, z, t) + (1 - \gamma) U_{\text{ref}} \quad (4)$$

$$T_{\text{inlt}}^{\text{outer}}(\eta_{\text{inlt}}) = \gamma T_{\text{recy}}(\eta_{\text{inlt}}) + \gamma_1 T'_{\text{recy}}(\eta_{\text{inlt}}, z, t) + (1 - \gamma) T_{\text{ref}} \quad (5)$$

$$V_{\text{inlt}} = V_{\text{recy}} \quad W_{\text{inlt}} = W_{\text{recy}} \quad (6)$$

where $\gamma = \frac{U_{\tau,\text{inlt}}}{U_{\tau,\text{recy}}}$, $\gamma_1 = 1$. The subscripts inlt and recy stand for the inlet plane and recycling plane, respectively. The superscripts inner or outer correspond to the inner or outer part of boundary layer, respectively. Since Lund et al. [4] used a fixed recycling plane, γ was a function of the distance between the recycling station and inlet, which was fixed in their method. In this paper, we suggest the following way to assign the value of γ . When the recycling plane is moving, $U_{\tau,\text{recy}}$ is calculated step by step, and $U_{\tau,\text{inlt}}$ is assigned to be the desired inlet skin friction velocity. When the recycling plane reaches the desired station, Lund et al.'s [4] γ is applied. Our numerical simulation shows that, after many recycling and rescaling operations, it is possible to underproduce or overproduce the rms fluctuations. This feature may result from modeling, the numerical scheme, or both. In this paper, we only consider the influence of the numerical method and the modeling issue will not be discussed. Usually, even order schemes are utilized in the simulation of turbulence because of their robustness and accuracy. However, the numerical errors associated with the even order schemes are dominated by dissipation. Note that the dissipation in the numerical simulation contains three parts: viscous, numerical, and modeling dissipation. In the design of a numerical simulation method, the dissipation of the method should be considered. In this sense, a well-chosen γ_1 can provide a remedy for this under or over production. We tested different values of γ_1 , including $\gamma_1 = \gamma$. Our experiences indicated that, when $\gamma_1 = 1$, the rms profiles matched well with Degraaff and Eaton's [9] experimental results using the fully implicit LES scheme.

In order to maintain the continuity of the inflow conditions, a weighting function, W , is proposed to combine the inner and the outer part of velocity and temperature profiles so that:

$$U(y_{\text{inlt}}^+) = U_{\text{inlt}}^{\text{inner}}(y_{\text{inlt}}^+)W(y_{\text{inlt}}^+) + (1 - W(y_{\text{inlt}}^+))U_{\text{inlt}}^{\text{outer}}(y_{\text{inlt}}^+)$$

$$T(y_{\text{inlt}}^+) = T_{\text{inlt}}^{\text{inner}}(y_{\text{inlt}}^+)W(y_{\text{inlt}}^+) + (1 - W(y_{\text{inlt}}^+))T_{\text{inlt}}^{\text{outer}}(y_{\text{inlt}}^+)$$

Since the law of the wall is only valid in the inner part of boundary layers and the defect law is only valid in the outer part, an improper weighting function may deform the profiles and cause the inflow rescaling to fail. Considering that the law of the wall and the defect law overlap in the logarithmic layer, we suggest the following weighting function:

$$W(y^+) = 1.0, \quad \text{when } y^+ < 50$$

$$W(y^+) = \frac{1}{2} \left[1.0 - \tanh \left(\frac{a(q-b)}{(1.0-2b)q+b} \right) \right] / \tanh(a), \quad \text{otherwise}$$

$$W(y^+) = 0, \quad \text{when } y^+ > 300$$

where $a = 0.5$, $b = 0.4$ and $q = (y^+ - 50)/(250)$. The above weighting function maintains the law of the wall or the defect law for $y^+ < 50$ or $y^+ > 300$, respectively. Only in the logarithmic region are the profiles composite.

3. Results and conclusions

In order to evaluate this inflow method, turbulent boundary layers ranging from $Re_d = 1850$ up to $Re_d = 2250$ were calculated by two different numerical schemes, a fully implicit scheme [12] and a semi-implicit scheme [13], where Re_d is the Reynolds number based on displacement thickness. The former scheme was a second order central difference LUSGS finite volume scheme, and the time difference was represented by a second order Euler backward scheme. The numerical procedure included two loops: inner loop and outer loop, (or pseudo time step and physical time step). Newton iteration was applied in the inner loop. The latter scheme was a four stage Runge–Kutta scheme. The convective terms were discretized by the Crank–Nicolson method. Second order central differences were utilized for the spatial discretizations. For both methods, random fluctuations were used to generate the initial fluctuation field, the convective boundary condition [4] was applied at the outflow boundary, and a dynamic subgrid-scale model proposed for compressible turbulence by Moin et al. [10] and recommended by Lilly [11] was implemented. The numerical mesh was $280 \times 80 \times 120$ in the streamwise, normal, and spanwise directions, respectively. The computational domain was $84 \times 30 \times 14.4$ in terms of distance normalized by the inlet displacement thickness. The Mach number was 0.06. The numerical time step was $0.2 \frac{\delta_d}{U_\infty}$. $\Delta y_{\min}^+ = 0.54$, $\Delta z^+ = 13.2$, and $\Delta x^+ = 33.0$. An adiabatic wall temperature condition was applied.

The LUSGS scheme [12] was found to be more efficient than the Runge–Kutta scheme and performed more accurately with the present rescaling procedure for the simulation of compressible flows. Thus, only the LUSGS results are presented in the figures to follow except for Fig. 4, where results from both methods are shown.

Fig. 1 compares the LES rms results with the DNS profiles obtained by Spalart [3], and the experimental profiles obtained by Degraaff and Eaton [9]. Fig. 2 shows a comparison of the mean streamwise velocity profile with the same DNS data and experimental data. The agreement is generally good.

The comparison of skin friction is shown in Fig. 3. In this figure, the solid line was obtained by the method proposed in this paper, and the dashed line shows the results obtained by using the same rescaling treatment but with a fixed recycling station at $X = X_{\text{tag}}$, which is $40\delta_d$, and the empirical curve is the Ludwig–Tillmann correlation. Both the solid and the dashed lines represent the average from $t = 100 \frac{\delta_d}{U_\infty}$ to $t = 300 \frac{\delta_d}{U_\infty}$. We also found that Lund et al.'s [4] suggestion for the starting transients works for the semi-implicit Runge–Kutta

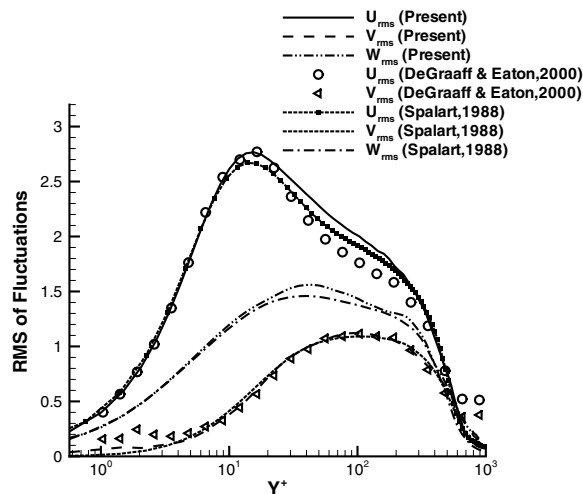


Fig. 1. Comparison of rms profiles by present method in a turbulent boundary layer $Re_{\delta_d} = 2000$ and zero free stream turbulence with the DNS data reported by Spalart [3] and the experimental data reported by Degraaff and Eaton [9].

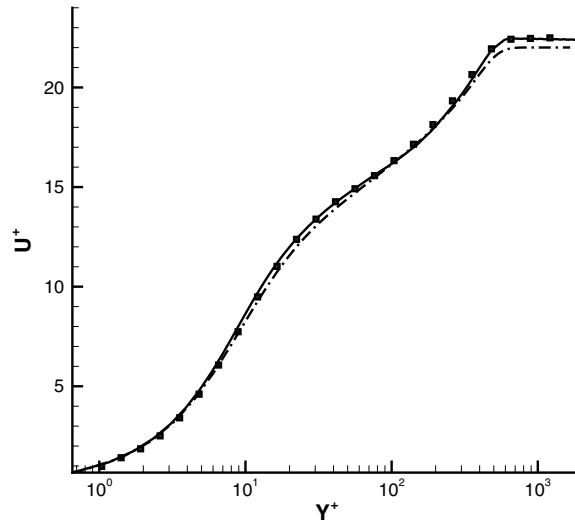


Fig. 2. Comparison of mean streamwise velocity distributions in a turbulent boundary layer $Re_{\delta_d} = 2000$. The solid line presents LES results, the dashed line gives the DNS profile obtained by Spalart [3], and the square symbols are experimental data reported by Degraaff and Eaton [9].

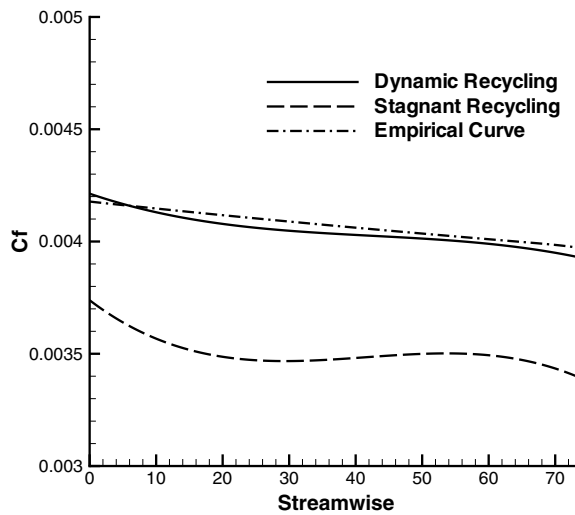


Fig. 3. Evolution of skin friction: —, recycling plane was dynamically chosen by Eq. (1); - - -, recycling plane was fixed; — · —, empirical curve is the Ludwig–Tillmann correlation.

scheme, but need to be improved for the fully implicit scheme because the starting transients are numerical phenomena relevant to the numerical scheme. The detailed information about the influence of initial conditions, boundary conditions, and numerical schemes on the starting transients still remains elusive. Considering that the maximum numerical time we calculated was only up to $t = 800 \frac{\delta_d}{U_\infty}$ which is shorter than Lund et al.'s [4] simulation, it is still possible that the skin friction by the fully implicit schemes could be recovered by Lund et al.'s [4] method after a longer simulation. But, the present dynamic recycling method can adjust the skin friction for both of the schemes within a short starting transient. This feature is illustrated in Fig. 4, which shows the time evolution of the skin friction at the station $X = 40\delta_d$. In Fig. 4, cases 1 and 3 were calculated by the fully implicit scheme, and cases 2 and 4 were calculated by the Runge–Kutta scheme. Lund et al.'s [4]

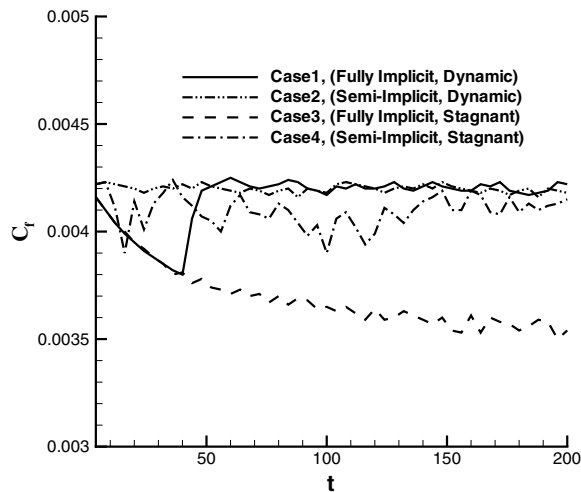


Fig. 4. Evolution of spanwise average skin friction coefficient at the station $X = 40\delta_d$ with time, where t is normalized by $\frac{\delta_d}{U_\infty}$.

suggestion for the starting transients [4] was utilized for cases 3 and 4, and the dynamic recycling method was utilized for cases 1 and 2.

In conclusion, this proposed dynamic recycling procedure shows good performance in establishing the correct skin friction. The method reduces the start-up transient and maintains a relatively short inlet buffer zone. Furthermore, a change was suggested to Lund et al.'s [4] inflow condition, which modifies the inflow fluctuations providing improved levels of the rms profiles according to our simulation.

Acknowledgments

This research was partially supported by Air Force Office of Scientific Research through Grant F49620-01-1-0113 and the National Science Foundation through Grant CTS-9806989.

References

- [1] M.M. Rai, P. Moin, Direct numerical simulation of transition and turbulence in a spatially evolving turbulence, *J. Comput. Phys.* 109 (1993) 169.
- [2] J.U. Schlüter, H. Pitsch, P. Moin, On boundary conditions for LES in coupled simulations, *AIAA Paper 0069*, 2003.
- [3] P.R. Spalart, Direct numerical simulation of turbulent boundary layer up to $Re_\theta = 1410$, *J. Fluid Mech.* 187 (1988) 61.
- [4] T.S. Lund, X. Wu, K.D. Squires, Generation of turbulent inflow data for spatially-developing boundary layer simulation, *J. Comput. Phys.* 140 (1998) 233.
- [5] A. Spille-Kohoff, H.-J. Kaltenbach, Generation of turbulent inflow data with a prescribed shear-stress profile, in: 3rd AFOSR Conference, Arlington, TX, 2001, p. 319.
- [6] S.E. Guarini, R.D. Moser, K. Shariff, A. Wray, Direct numerical simulation of a supersonic turbulent boundary layer at Mach 2.5, *J. Fluid Mech.* 414 (2000) 1.
- [7] C.R. Smith, S.P. Metzler, The characteristics of low-speed streaks in the near-wall region of a turbulent boundary layer, *J. Fluid Mech.* 129 (1983) 27.
- [8] Y. Iritani, N. Kasagi, M. Hirata, Heat transfer mechanism and associated turbulent boundary structure in the near-wall region of a turbulent boundary layer, in: L.J.S. Bradbury, F. Durst, B.E. Launder, F.W. Schmidt, J.H. Whitelaw (Eds.), *Turbulent Shear Flows*, vol. 4, Springer-Verlag, Berlin, 1985, p. 223.
- [9] D.B. DeGraaff, J.K. Eaton, Reynolds-number scaling of the flat-plate turbulent boundary layer, *J. Fluid Mech.* 422 (2000) 319.
- [10] P. Moin, K. Squires, W. Cabot, S. Lee, A dynamic subgrid-scale model for compressible turbulence and scalar transport, *Phys. Fluids A* 3 (1991) 2746.
- [11] D.K. Lilly, A proposed modification of the Germano subgrid-scale closure method, *Phys. Fluids A* 4 (1992) 633.
- [12] X. Xu, J.S. Lee, R.H. Pletcher, A compressible finite volume formulation for large eddy simulation of turbulent pipe flows at low Mach number in Cartesian coordinates, *J. Comput. Phys.* 203 (2005) 22.
- [13] L.D. Dailey, R.H. Pletcher, Evaluation of multigrid acceleration for preconditioned time-accurate Navier–Stokes algorithms, *Comp. Fluids* 25 (8) (1996) 791.